

Presented at Fourth Int.  
Congress of the IRPA,  
Paris, April 1977

ISTITUTO NAZIONALE DI FISICA NUCLEARE  
Laboratori Nazionali di Frascati

LNF-77/12(P)  
24 Aprile 1977

A. Esposito, F. Lucci and M. Pelliccioni: ON THE DISTRIBUTION  
OF THE RADIATION DOSES FROM THICK TARGETS IN HIGH  
ENERGY ELECTRON ACCELERATORS.

A. Esposito, F. Lucci<sup>(x)</sup> and M. Pelliccioni: ON THE DISTRIBUTION OF THE RADIATION DOSES FROM THICK TARGETS IN HIGH ENERGY ELECTRON ACCELERATORS<sup>(o)</sup>.

**ABSTRACT. -**

In the present paper some general properties of electromagnetic cascade showers are reviewed which can be used to have rough estimates of radiation doses around thick target in high energy accelerators. Some direct experimental results on dose distribution produced by high energy electron or bremsstrahlung beams striking thick targets are discussed from the health physics point of view. Finally few examples are presented, in which the said informations are employed to solve some operational health physics problems around the Frascati accelerators.

**1. - INTRODUCTION. -**

Any massive object on which a high energy beam targets constitutes an important source of secondary radiations. The knowledge of this radiation field, its nature and its angular distribution is of high interest for various health physics respects, including shielding calculations and dose estimates for accidental overexposures.

For the electron accelerators we must consider electron or bremsstrahlung beams. In both cases an electromagnetic cascade shower is produced in the target with the consequent photoproduction of several particles, mainly neutrons and protons and, if it is energetically possible, pions and  $\mu$  mesons. Anyhow the principal contribution to the radiation doses near the targets will be always due to the electromagnetic component and to a lower extent, to the neutrons. In this paper we are mostly interested to poor shielding situations and so only the electromagnetic component will be considered.

---

(x) - CNEN, Centro di Frascati.

(o) - Presented at Fourth Intern. Congress of the IRPA, Paris, April 24-30, 1977.

In the next some general properties of electromagnetic cascade showers will be pointed out, which can be usefully employed to obtain some knowledge about the radiation fields near thick targets.

Several experimental results will be also discussed. Finally we intend to present few examples of utilization of the said informations to solve some operational health physics problems around the Frascati accelerators.

## 2. - GENERAL DESCRIPTION OF ELECTROMAGNETIC CASCADE SHOWERS. -

It is known that, though the basic electromagnetic interactions of the electrons and photons are well understood, it is very difficult to describe satisfactorily the entire shower development.

Among the theoretical studies we can mention the one-dimensional analytical theory by Rossi and Greisen<sup>(1)</sup> and the Monte Carlo calculations performed by several authors<sup>(2-4)</sup>.

It must be noted that the calculations of Rossi and Greisen because of their own nature (one-dimensional approximation) cannot account for the radial development of the shower. Furthermore all the analytical methods introduce several oversimplifications, which do not take accurately into account the low energy particles and seem to be inadequate to describe the behaviour at great depths.

The most useful informations about radial and longitudinal development at great depths can be obtained by a critical comparison of the Monte Carlo results with the experimental data.

If we consider first the longitudinal development as described in the experimental works by several authors<sup>(5-11)</sup>, we note that both the dose at the axis and the transition curve (which is obtained by integration of the lateral distribution from  $r = 0$  to  $r = \infty$ ) decrease beyond the shower maximum approximately like an exponential. The experimental coefficient  $\lambda_{exp}$  of this exponential is a very significant datum, as it was discussed by several authors<sup>(5, 7, 9, 10, 11)</sup>. Table I shows

TABLE I - Comparison of the experimental coefficient  $\lambda_{exp}$  with the minimum values of the attenuation and absorption coefficients.

Material	$\lambda_{min}$ (cm <sup>2</sup> /g)		$\lambda_{exp}$ (cm <sup>2</sup> /g)
	Attenuation	Absorption	
Water	0.0150	0.0140	0.0130 (5)
Aluminium	0.0215	0.0183	0.0187 (5)
			0.0156 (6)
			0.0160-0.0164 (7)
Copper	0.0303	0.020	0.026 (6)
			0.028 (8)
			0.024 (9)
			0.029 (10)
			0.028-0.029 (7)
Tin	0.0355	0.022	0.033 (10)
Lead	0.018	0.028	0.041 (6)
			0.043 (8)
			0.045 (9)
			0.0435 (10)
			0.046-0.047 (7)
Concrete	0.0209	0.017	0.020 (11)
Heavy Concrete	0.025	---	0.019 (8)

$\lambda_{exp}$  for various materials and the related minimum values of the attenuation and absorption coefficients. It follows from the comparison that  $\lambda_{exp}$  normally falls between the minima of the two theoretical coefficients and that for low atomic numbers it approaches the absorption one, while for heavy elements it tends to agree with the minimum attenuation coefficient.

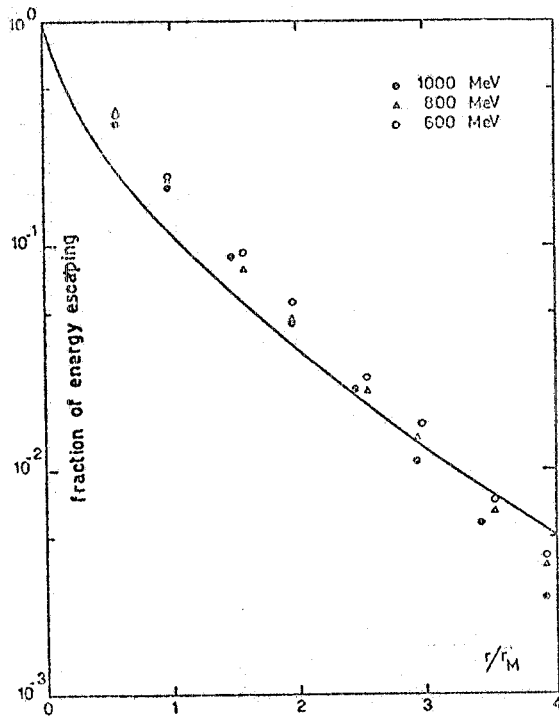
The said circumstance permits to deduce that the electromagnetic shower penetration at great depths is mainly controlled by photons whose energy lies near the minimum of the attenuation curve and that, in equilibrium with this component there are lower energy secondaries which are stopped more quickly. This conclusion is, of course, of great interest from the health physics point of view because it provides useful indications on the energy spectrum of the secondary radiations from thick targets.

This model was directly confirmed by an experiment which was performed at the Frascati Electrosynchrotron measuring the doses on the beam axis in a concrete absorber with several lead slabs placed in front of it<sup>(11)</sup>. Table II shows the experimental slopes of the exponential tail in the concrete versus the lead thickness. As can be easily seen, the thicker is the lead slab, the closer is the experimental slope to the attenuation coefficient in concrete of the most penetrating  $\gamma$ -rays in lead ( $0.032 \text{ cm}^2/\text{g}$  at 4 MeV).

The said model is also confirmed by some measurements which were made at Stanford to study the absorption in lead of the photon radiation coming from an iron target on which a 12 GeV electron beam was impinging. The experiment was conducted at three angles ( $0^\circ$ ,  $45^\circ$  and  $90^\circ$ ) respect to the beam direction and an absorption coefficient of  $0.047 \text{ cm}^2/\text{g}$  was always found, which corresponds very well to the attenuation coefficient in lead of 8 MeV  $\gamma$ -rays, i. e. of the most penetrating  $\gamma$ -rays in iron.

TABLE II - Experimental slopes of the exponential tail, in attenuation measurement in lead and concrete absorbers.

Thickness of lead (cm)	Slope ( $\text{cm}^2/\text{g}$ )
5	0.024
10	0.026
20	0.029



Another useful characteristic for the evaluation of gamma doses around thick targets has been suggested by Nelson et al.<sup>(9)</sup>. Following these authors the fraction of the total energy escaping from an infinitely long cylinder, with its axis parallel to the beam, only depends from the radius measured in Molière units<sup>(x)</sup>, irrespective of the energy of the incident beam and of the target material.

Both the Monte Carlo results<sup>(2-4)</sup> and the experiments conducted by several authors (refs. 7, 9, 11, 13) agree quite well with the said property. Fig. 1 shows, for example, the results obtained at Frascati with a 1000 MeV bremsstrahlung beam targetting on an ordinary concrete absorber. Only Crannel's data<sup>(5, 10)</sup> show a sensibly slower decrease with the radius.

Fig. 1 - Radial escaping curve for 1 GeV bremsstrahlung beams on concrete. The solid curve refers to the Monte Carlo results by Nagel<sup>(4)</sup>.

(x) - The Molière unit is defined by  $X_m = X_0 E_s / \epsilon_0$ , where  $\epsilon_0$  is the critical energy,  $X_0$  the radiation length and  $E_s = 21.2 \text{ MeV}$ .

This effect is larger the lower the atomic number of the absorber and probably can be related with the high sensitivity of the Crannel's CsI detector to the low energy  $\gamma$ -rays<sup>(7)</sup>.

In the case of a thick target with transversal size of some Molière units, it is clear that it should be possible to obtain some rough but useful evaluations of doses around the target, by using the two said circumstances and supposing the radially escaping energy as radiated isotropically. The evaluation of the small angle doses are of course very difficult and no simple way to do it can be suggested, provided that they are too dependent on the particles energy and the geometric characteristic of the beam (i. e. size and divergence).

### 3. - EXPERIMENTAL DATA ON DOSE DISTRIBUTION AROUND THICK TARGETS. -

Often it is not sufficient to resort to simple considerations of the type we have already exposed. Recourse is then needed to theoretical calculations, which can be quite complexe, or to direct experimental results. So it can be useful to review those between the available results that are easier to employ for radioprotection purposes.

A very detailed study on 20, 30 and 100 MeV electrons striking tantalum targets was conducted by Wyckoff et al.<sup>(14)</sup> at the NBS linear accelerator. In Fig. 2 we have reported the angular distribution of doses measured by these authors at a depth of 4.5 g/cm<sup>2</sup> in a tissue-equivalent phantom. The transversal dimensions of the target were 6.2 x 7.7 cm<sup>2</sup>, with a thickness depending from the energy (12.9 g/cm<sup>2</sup> at 20 MeV; 21.46 g/cm<sup>2</sup> at 30 MeV; 67.92 g/cm<sup>2</sup> at 100 MeV). The behaviour for angles greater than 20° does not strongly depend from the energy, at least if the 100 MeV curve is excluded, which according to the authors must be treated with considerable skepticism at angles greater than 30°.

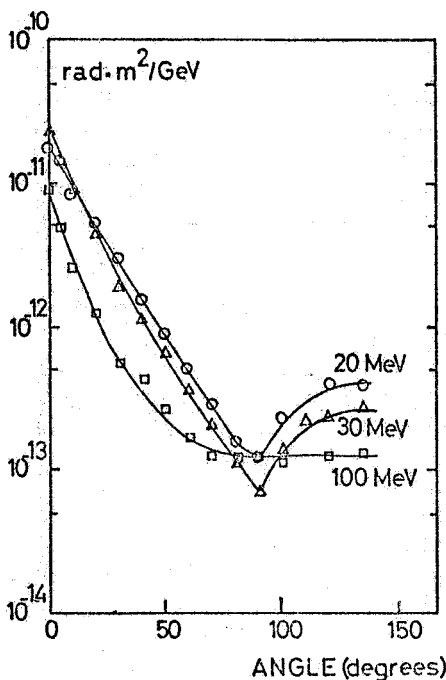


Fig. 2 - The angular distribution of dose as measured at a depth of 4.5 g/cm<sup>2</sup> in a polymethylmethacrylate phantom, for the cases of 20, 30 and 100 MeV electrons incident on targets of various thicknesses (modified from Wickoff et al.<sup>(14)</sup>).

In particular one can note the self-absorption minimum of about 10<sup>-13</sup> rad·m<sup>2</sup>/GeV at 90°. Now, if an attempt is made to evaluate the 90° dose with the criteria introduced in the previous paragraph, a value is obtained falling between about 1.6 x 10<sup>-14</sup> and 3.7 x 10<sup>-14</sup> rad·m<sup>2</sup>/GeV, depending on the various possible hypothesis on the geometry of the exposure. The agreement is satisfactory.

If higher energy electrons are concerned, we can mention some measures carried out at Stanford respectively with 7 GeV electrons striking a typical copper absorber (15.6 X<sub>0</sub> long, 2.7 X<sub>m</sub> radius) and with 0.99 GeV electrons on an iron absorber (21.4 X<sub>0</sub> long, 4.1 X<sub>m</sub> radius). The experimental angular distribution is shown in Fig. 3. In these cases too the measured values can be compared with the mean doses computed for great angles second the said criteria, i. e. 4.4 x 10<sup>-14</sup> rad·m<sup>2</sup>/GeV for the 7 GeV iron case and 1.9 x 10<sup>-14</sup> rad·m<sup>2</sup>/GeV for the 0.99 GeV copper case.

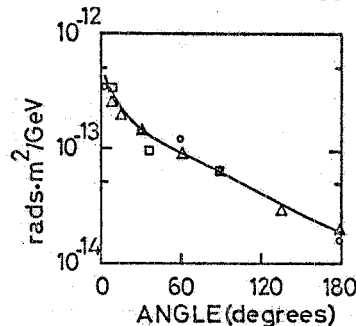


Fig. 3 - Experimental angular distribution of dose around typical absorbers, in the case of 7 GeV electrons on copper or 0.99 GeV electrons on iron (modified from Stanford data<sup>(12)</sup>).

Similar measurements have also been carried out at Frascati with a 1 GeV bremsstrahlung beam striking lead or tungsten targets of various thicknesses<sup>(15)</sup>. In this experiment the measurements were performed by means of termoluminescent LiF dosimeters, which were inserted in polyethylene phantoms at the following depths: 0, 2.5, 5.0, 7.5 and 10 cm. The target thicknesses were 0.4 mm, 3.4 mm, 9.2 mm, 11.8 mm, 14.8 mm and 25.6 mm for the tungsten; 86 mm and 123 mm for the lead case. Their lateral dimensions were always 5 x 5 cm<sup>2</sup>.

The results for W targets are shown in Fig. 4, while Fig. 5 refers to those for the two Pb targets.

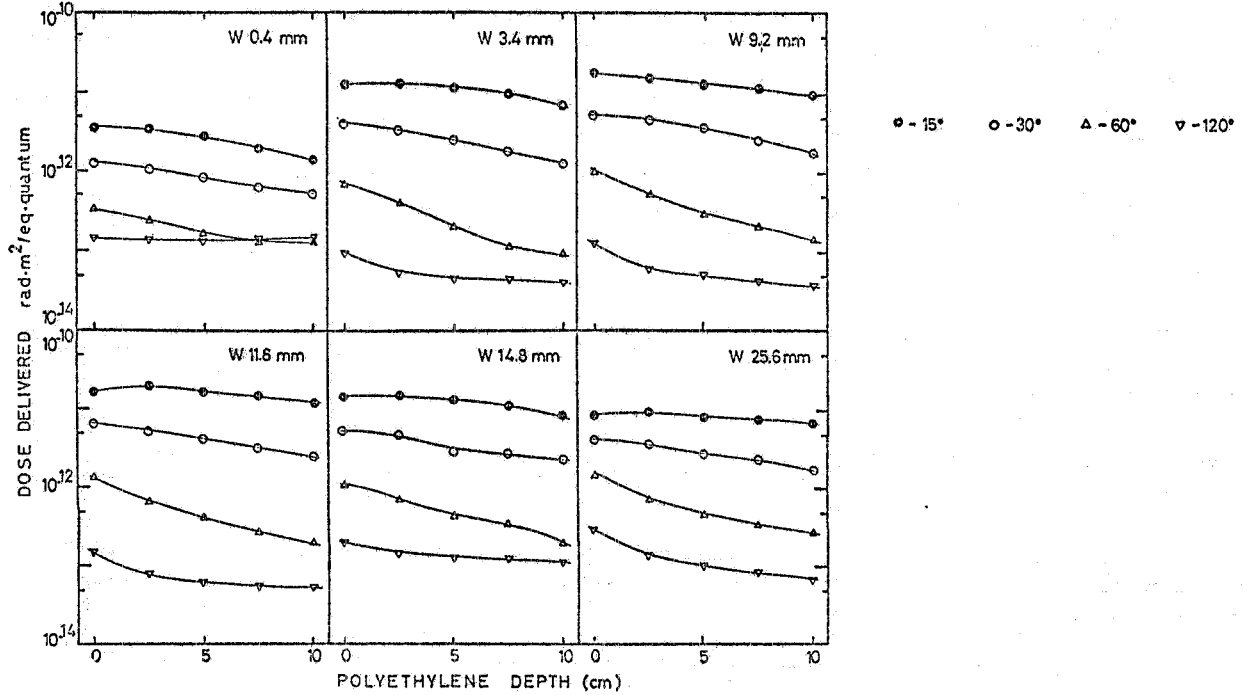


Fig. 4 - Dose distribution measurements in the case of a 1 GeV bremsstrahlung beam striking W targets of various thicknesses. The data are presented as depth dose curves in polyethylene for some fixed angles relative to the beam direction.

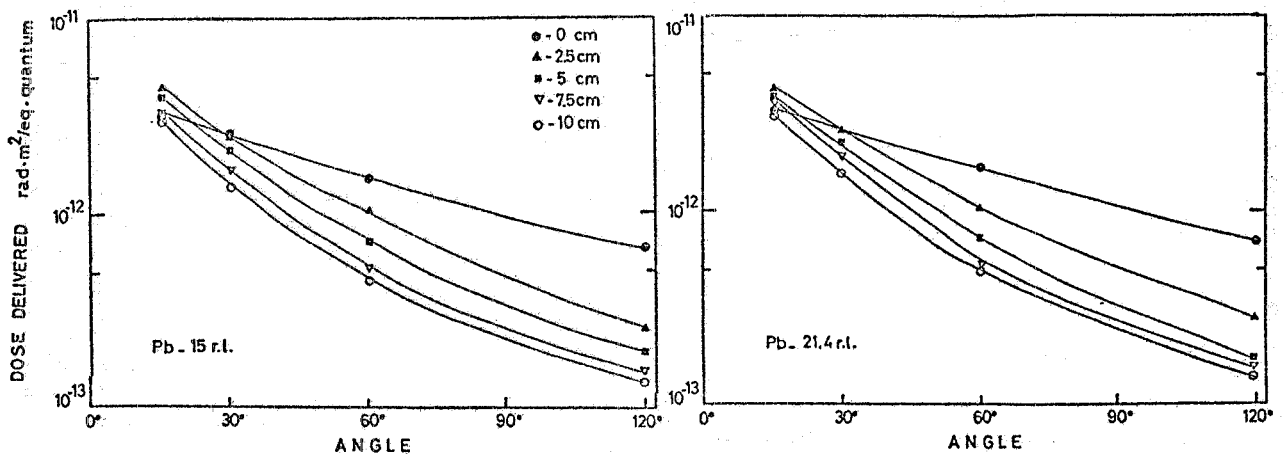


Fig. 5 - Dose distribution measurements in the case of a 1 GeV bremsstrahlung beam striking Pb targets of two thicknesses. The data are presented as angular distribution of dose measured at various polyethylene depths.

the beam dump placed at 2-3 m from the polyethylene phantoms. The amount of this contamination has been found to be unimportant except for the measurement performed using thin targets. For example, for a W target 0.4 mm thick, the doses measured at angles of  $60^\circ$  and  $120^\circ$  coincide with the background while the data at  $15^\circ$  and  $30^\circ$  show a contamination of about 15%. Increasing the target thickness the background contamination decreases. We can estimate that, for the 2.4 mm target, only the measurements at  $60^\circ$  and  $120^\circ$  are effected, while for greater thicknesses the background can be disregarded.

The main characteristic of the experimental curves in Fig. 4 is the strong dependence of their behaviour on angle. In fact the small angle curves show a broad maximum and then decrease with increasing phantom depth while the large angle ones are always decreasing. This circumstance, which is evident also from the Pb results, though they have not been plotted versus the polyethylene depth, can be explained assuming that high energy particles contribution dominates in the forward direction, while the low energy particles are predominant at large angles.

Of course, for a fixed depth in the phantom, the dose decreases strongly for increasing angles. For thick targets this angular anisotropy is less evident. In fact the fraction of the shower absorbed in the target increases, thus decreasing the dose at small angles. On the other hand the wide angle contribution, which is due mainly to the limited transverse dimension of the target (the same for all thicknesses), stays practically constant.

Furthermore we point out that the doses at  $60^\circ$  and  $120^\circ$  are consistent with the values computed according the previous model ( $4.8 \times 10^{-14}$  rad.  $m^2/GeV$  for the W targets and  $1.5 \times 10^{-13}$  rad.  $m^2/GeV$  for the Pb case).

The data for zero depth are also shown in Fig. 6 as function of the target (W) thickness expressed in radiation length. The figure shows that the maximum dose normally corresponds to a thickness equal to the maximum shower development ( $\approx 3.36$  r.l.), as foreseen by the shower theory.

Qualitatively our bremsstrahlung curves are similar to those found by Wyckoff. A quantitative comparison is not possible because the two experiment use different particles and energies. However, one can note that the order of magnitude of the doses is not so different as the different

experimental conditions would suggest. In detail, our small angle values, if normalized to the total energy incident on the target, are about 10 times higher than those found by Wyckoff at 100 MeV, while the two experiments give similar values at large angles. The first observation can be explained with the higher energy of our beam. On the other hand, the similarity of the wide angle results can be related to the transverse dimensions of the targets expressed in Molière lengths which were quite similar in both cases.

At last we wish remember an experiment performed at Stanford by Jenkins et al. (16) with the purpose of obtaining some data which were needed for the design of shielding for SPEAR. In this experiment such targets and geometries were chosen as to well simulate the losses of electrons on the accelerator structures. Fig. 7 shows partially and with modified units the results obtained by the said authors for the case of 2 GeV electrons targetting at small angles on a thick iron plate and on thin aluminium one.

A discussion of these results is not our aim and it can be found in the original note. However we wish emphasize the usefulness of such type of experimental results for the practical radioprotection work around high energy electron accelerators.

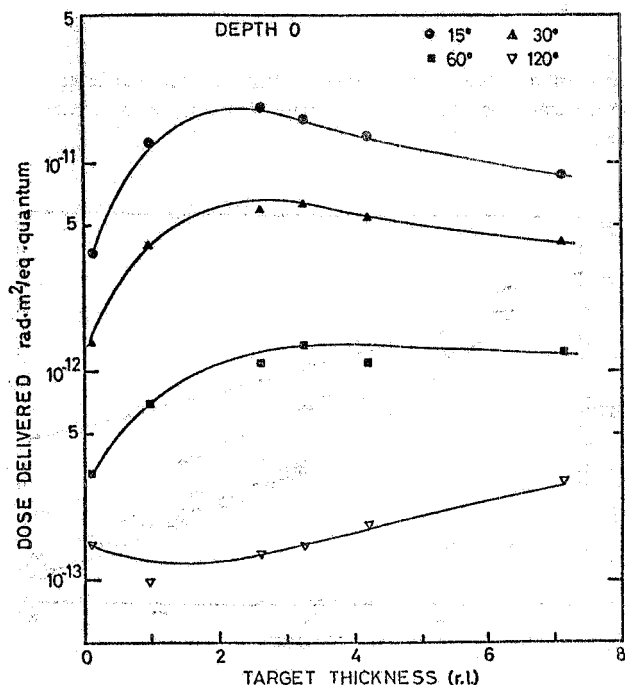


Fig. 6 - Variation of the dose measured at zero polyethylene depth with the target thickness, for the same data of Fig. 4.

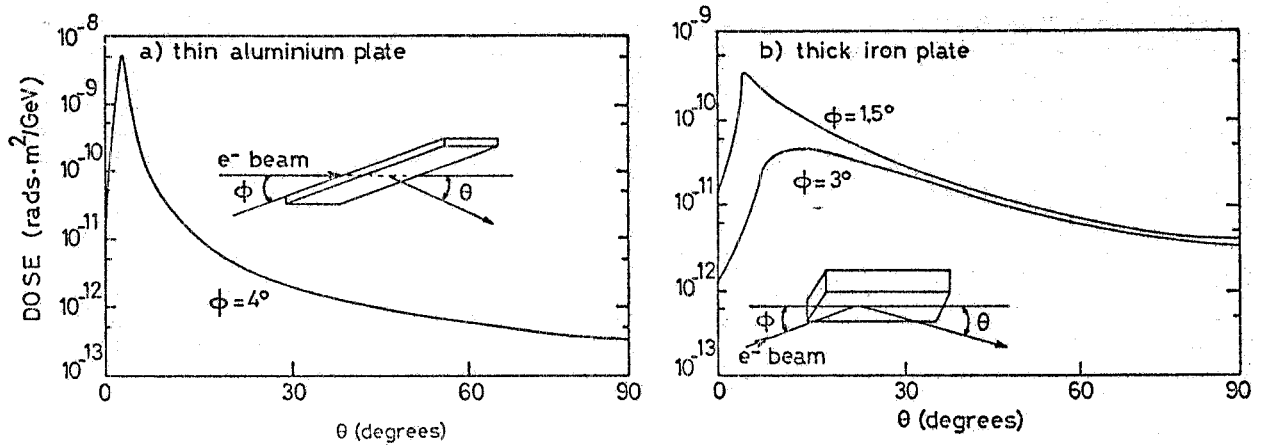


Fig. 7 - Angular distribution of radiation from a thick iron plate and a 0.25 inch aluminium plate struck by a 2 GeV electron beam at small angles (heavily modified from T. M. Jenkins et al.<sup>(16)</sup>).

4. - SOME EXAMPLE OF APPLICATION TO OPERATIONAL PROBLEMS. -

Lastly it is quite interesting to examine some examples of application of the exposed notions to some operational health physics problems around high energy electron accelerators.

The most direct case is of course the design of biological shielding around thick targets, such as can be considered the beam dumps or some structures of the machine on which a significant beam loss is expected. However we shall not dwell on this aspect because the application of the data and the notion which were furnished in the previous paragraphs is quite immediate. Besides when this is not sufficient, complexe calculations are needed which do not come in our matter.

Another question is the evaluation of radiation doses without shielding or in some situation of poor shielding. This is an important matter for the estimate of accidental overexposures or for the planning of the operations in some particular areas, like the Adone ring, during stored beam operation. In both the said cases, the electromagnetic component is the main one in the radiation field, while the neutrons can be relevant or also sometimes dominant for shielding calculations.

As far as the evaluation of accidental exposures is concerned, we can suppose that a man would stay few minuts near a part of the machine acting like a thick target. If the beam strikes the target normally it is of course easy to employ the previously reported data if available. As an example we can consider a bremsstrahlung beam hitting normally a tungsten target with an intensity of  $10^{10}$  equivalent quanta per second. In this case the dose that would be absorbed by a man staying 2 minuts at a distance of 50 cm from the target can be evaluated from Figg. 4 and 6. The results are shown in Table III for various angles respect to the beam direction. Moreover we point out the dose at  $90^\circ$  can be lower and it depends mostly from the lateral size of the target.

TABLE III - Doses by accidental exposure 0.5 m away from a W target struck by a 1 GeV bremsstrahlung beam (intensity  $10^{10}$  equivalent quanta/sec; exposure time 2').

Angle respect the beam (degrees)	Normalized dose (rad. m <sup>2</sup> /GeV)	Accidental dose (rad)
15°	2.0 x 10 <sup>-11</sup>	95
30°	6.7 x 10 <sup>-12</sup>	32
60°	1.4 x 10 <sup>-12</sup>	7
120°	3.0 x 10 <sup>-13</sup>	1.5

The previous case has the peculiarity of a very simple geometry with a point source which is well localized. However practical cases are often more complexe, with a distribution of the losses which cannot be "a priori" well understood and with small angles of incidence. As an example we can cite the case of the 1 GeV extracted beam



of the Frascati Electrosynchrotron. The 2 GeV data of Fig. 7 will be used to tray an order of magnitude evaluation of the dose rates at 25 cm of distance from a point on which about 1% of the beam current (about  $10^{10}$  e/s) is lost. If a lower angle than  $15^\circ$  can be excluded, a normalized dose falling between  $5 \times 10^{-12}$  and  $5 \times 10^{-11}$  rad.  $m^2/GeV$  can be adopted for the thick target case. For thin targets a ten times lower value can be expected. So in the said hypothesis the dose rates around the beam line will fall between 0.5 and 5 rad/min for thick targets and between 50 and 500  $\mu$ rad/min for thin targets.

Now to have an evaluation for the real case it would be of course necessary the knowledge of the distribution and of the greatness of the beam losses. Fig. 8a shows the radiation levels from induced radioactivity which were measured along the beam pipe just after the machine shutdown. These values can furnish a picture of the distribution of losses. In Fig. 8b we indicate the doses measured in the same conditions during 8 minutes of machine operation. If the data reported in Fig. 8b are compared with the previous evaluation, one can see that measured doses are consistent with a loss of few per cent of the beam current distributed mostly between the pairs of quadrupoles 5-6 and 7-8.

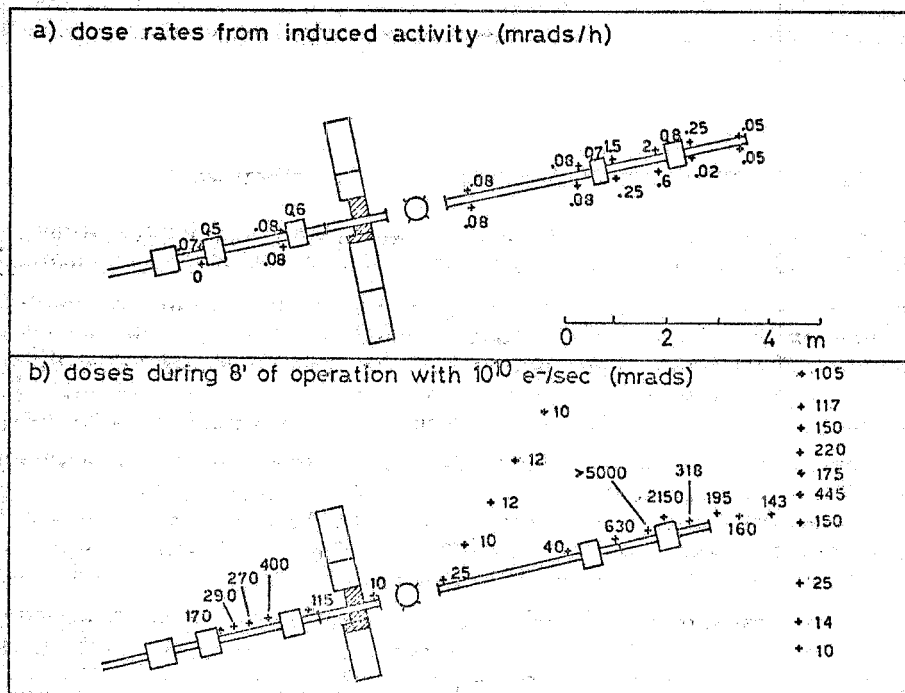


Fig. 8 - a) Dose rates from induced activity around the beam pipe of the 1 GeV extracted beam at the Frascati Electrosynchrotron just after the shutdown; b) Measured doses around the same beam pipe during 8 minutes of operation.

A last example of application of the data in Fig. 7 is the evaluation of the doses near the storage ring Adone in the case of a sudden loss of the stored beams. The aim of such an evaluation is to permit few researchers to stay near the ring during stored beam operation. In fact this type of operations cannot be "a priori" excluded, owing to the finite number of circulating particles and to the low rate of losses in the normal operation<sup>(17)</sup>.

Because some hypothesis must be of course made on the distribution of the losses along the ring, we shall consider the two extreme cases on uniformly distribution and of a single point loss. The source strength was evaluated from data in Fig. 7, referring to the worst cases, i.e. the thick plate small angle ones. The geometry is shown in Fig. 9 where S is the source and P is the point of interest. The results of our calculation are shown in Fig. 10, versus the distance between the point of interest and the center of the ring. In the top of the figure we plotted the doses calculated assuming that the source radiates isotropically for all the angles greater than  $20^\circ$  with the same strength

which was measured at  $20^\circ$  by Jenkins et al.. The bottom of the same figure refers to the real angular distribution. All the dose values have been normalized to  $10^{11}$  electrons lost along the ring.

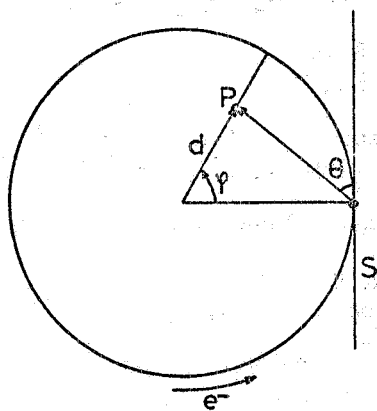


Fig. 9 - The geometry for the dose estimates near Adone in the case of a sudden loss of the stored beam.

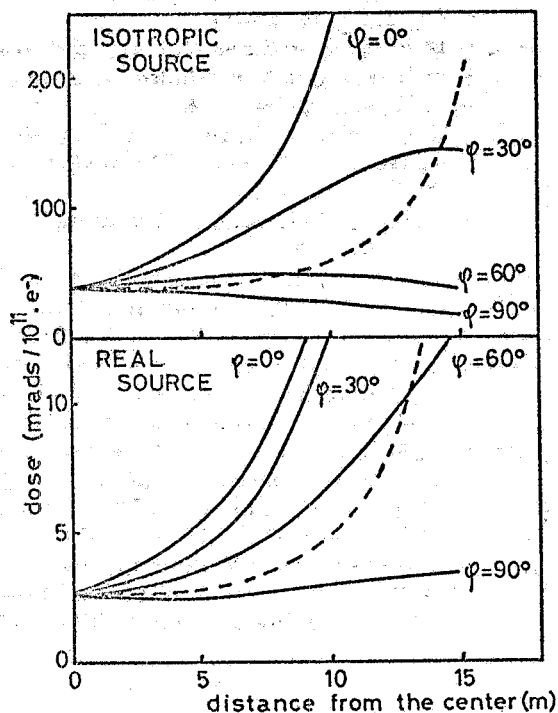


Fig. 10 - Calculated doses in the Adone hall in the cases of uniformly distributed losses (dashed curves) or point losses, for various azimuthal angles  $\varphi$ .

We note that in the second case the levels are found to be lower by about an order of magnitude than in the first one. Furthermore the distributed losses curves represent quite well in both cases the situation in the central area inside the ring, also when they are compared to the point losses curves with  $\varphi = 0^\circ$ , which is of course the worst case. In fact for both the types of losses the doses differ at most by a factor 4, if only distances from the center are considered which are smaller than 10 m.

The former evaluations are of course conservative, and in particular no attenuation for self-shielding or magnet-shielding was introduced. At last we want note that they agree with the results of many measurements carried out around Adone<sup>(18)</sup>. In fact no measurable values were found over 3m away from the ring, while close to the machine a maximum dose was found about  $4 \text{ rad}/10^{11}$  electrons.

REFERENCES. -

- (1) - B. Rossi, High Energy Particles (Prentice Hall, 1956); B. Rossi and K. Greisen, Rev. Mod. Phys. 13, 240 (1941).
- (2) - D. F. Crawford and H. Messel, Phys. Rev. 128, 2352 (1962).
- (3) - C. D. Zerby and H. S. Moran, J. Appl. Phys. 34, 912 (1965).
- (4) - H. H. Nagel, Zeits. Phys. 186, 319 (1965).
- (5) - C. J. Crannel, H. Crannel, R. R. Whitney and H. D. Zeman, Phys. Rev. 184, 426 (1969).
- (6) - G. Bathow, E. Freytag, M. Kobderberg, K. Tesch and R. Kajikawa, Nuclear Phys. 820, 592 (1970).
- (7) - T. Yuda, A. Masaike, A. Kusumegi, Y. Murata, I. Otha and J. Nishimura, Nuovo Cimento 65A, 205 (1970).
- (8) - G. Bathow, E. Freytag and K. Tesch, Nuclear Phys. B2, 669 (1967).
- (9) - W. R. Nelson, T. M. Jenkins, R. C. MacCall and J. K. Cobb, Phys. Rev. 149, 149 (1966).
- (10) - C. J. Crannel, Phys. Rev. 161, 310 (1967).
- (11) - F. Lucci, M. Pelliccioni and M. Rocella, Frascati report LNF-69/71 (1969).
- (12) - R. B. Neal (Ed.), The Stanford Two-Miles Accelerator (Benjamin, 1968).
- (13) - Y. Murata, J. Phys. Soc. Japan 20, 209 (1965).
- (14) - S. M. Wyckoff, J. S. Pruitt and G. Svensson, Proc. Intern. Congress on Protection against Accelerator and Space Radiation, CERN 71-16 (1971), Vol. 2, pag. 773.
- (15) - A. Esposito, F. Lucci and M. Pelliccioni, Nuclear Instr. and Meth. 138, 209 (1976).
- (16) - T. M. Jenkins, G. I. Warren and J. L. Harris, Report SLAC TN-70-34 (1970).
- (17) - F. Lucci and M. Pelliccioni, Frascati report LNF-75/49 (1975).
- (18) - M. Pelliccioni and M. Rocella, Proc. Intern. Congress on Protection against Accelerator and Space Radiation, CERN 71-16 (1971), Vol. 2, pag. 924.